ARTICLE IN PRESS

Discrete Applied Mathematics ▮ (▮▮▮▮) ▮▮▮–▮▮▮

Contents lists available at ScienceDirect

Discrete Applied Mathematics

journal homepage: www.elsevier.com/locate/dam

On the polyhedra of graceful spheres and circular geodesics

Ranita Biswas [a], Partha Bhowmick [a,*], Valentin E. Brimkov [b,1]

[a] Computer Science and Engineering Department, Indian Institute of Technology, Kharagpur, India

[b] Mathematics Department, SUNY Buffalo State, 1300 Elmwood Avenue, Buffalo, NY 14222, USA

ARTICLE INFO

Article history:
Received 2 April 2015
Received in revised form 2 August 2015
Accepted 30 November 2015
Available online xxxx

Keywords:
Graceful surface
Graceful sphere
Polyhedral surface
Discrete geometry
Discrete spherical geodesics
3D imaging

ABSTRACT

We construct a polyhedral surface called a *graceful surface*, which provides best possible approximation to a given sphere regarding certain criteria. In digital geometry terms, the graceful surface is uniquely characterized by its minimality while guaranteeing the connectivity of certain discrete (polyhedral) curves defined on it. The notion of "gracefulness" was first proposed in Brimkov and Barneva (1999) and shown to be useful for triangular mesh discretization through graceful planes and graceful lines. In this paper we extend the considerations to a nonlinear object such as a sphere. In particular, we investigate the properties of a discrete geodesic path between two voxels and show that discrete 3D circles, circular arcs, and Mobius triangles are all constructible on a graceful sphere, with guaranteed minimum thickness and the desired connectivity in the discrete topological space.

1. Introduction

In volume graphics, objects are represented by isothetic polyhedra composed by unit cubes (voxels) defined by the integer grid. In digital geometry for computer imagery and in combinatorial image analysis, such polyhedra are used to define discrete analogs of various Euclidean primitives (such as straight lines, planes, polygons, circles, or spheres), and obtaining an analytical description of a discrete object is highly desirable. In the present work, we introduce a new discrete model of a sphere and study its properties. Let us mention at this early point that at low-level image processing, digital objects and related properties and algorithms are usually represented and implemented in graph-theoretic terms, while in the scientific literature, for ease of understanding, these are traditionally given in terms of voxels and relations among them. In this paper, we conform to the latter paradigm.

As the sphere is a basic Euclidean primitive, a multitude of work on discrete spheres has been reported in the literature over the last two decades [1,3,5,19,11,15,16,14,21–23,27,35,34,36,42,43]. These are mostly of two types—one is on mathematical characterization of discrete spheres, and another is on voxelation techniques. Among those focused on voxelation, some are based on real specification and some on integer specification. In our work, we adopt an integer specification (i.e., integer radius and integer center) of the real sphere, which leads to an interesting and useful number-theoretic characterization of the resultant naive sphere, as recently shown in [6].

Another motivation for our study is found in possible applications in rapid prototyping (RP) technologies. With the advent of 3D imaging sciences and RP technologies, discrete spheres are widely used today for fabrication of different parts and products in diverse fields of science and technology, such as mechanical and electrical systems, microrobotics, biofabrication and bioprinting [18,25,26,28,30,31,33,41,45]. A series of work related to RP techniques in general, and 3D

* Corresponding author.
E-mail addresses: biswas.ranita@gmail.com (R. Biswas), pb@cse.iitkgp.ernet.in (P. Bhowmick), brimkove@buffalostate.edu (V.E. Brimkov).

[1] On leave from the Institute of Mathematics and Informatics, Bulgarian Academy of Sciences, Sofia, Bulgaria.

http://dx.doi.org/10.1016/j.dam.2015.11.017
0166-218X/

Please cite this article in press as: R. Biswas, et al., On the polyhedra of graceful spheres and circular geodesics, Discrete Applied Mathematics (2015), http://dx.doi.org/10.1016/j.dam.2015.11.017

printing in particular, has come up over the last few years to address and strengthen the theoretical underpinnings in the digital technology. The 3D building matter is treated as digital in the sense that the building block is a digital unit or *voxel*, as opposed to analog (continuous) material used in conventional RP. Further, as the printing device works in discrete steps with a precision governed by the control system and its degrees of freedom, the input domain effectively maps to the integer space. As the physical size of a printable voxel can be as fine as a few microns, the actual radius of a 3D-printed sphere is obtained by specifying the integer radius in voxel unit [17,28,29,38].

The use of spheres in discrete and polyhedral form is also gradually becoming prevalent in many other areas of science and engineering where computational issues need to be addressed; to name a few, these are medical science, computational fluid dynamics and turbulence modeling, and optical science. For example, in medical science, discrete spheres have been used in [37,44] for detection of pulmonary nodules and for medical analysis of brains. For aircraft navigation, a sphere voxelation technique is used in [39,40] to compute the minimum distance between a set of points and a discrete surface element, and is shown to be more efficient than other alternatives for minimum distance computation. In the field of applied optics, polyhedral approximation of spheres has been used in [46] to circumscribe agglomerated debris particles for experimentation and study of light scattering in the process of discrete dipole approximation.

Note that, unlike in Euclidean geometry, having and using unique definition of a discrete object is a very rare event. In fact, a number of definitions exist for each of the basic Euclidean primitives, as usually any definition has advantages and disadvantages to the others depending on the specific context and applications. For example, in the framework of arithmetic geometry,[2] discrete straight lines and discrete planes are well-studied—and also quite well-established by today—for their deep theoretical connections to imaging sciences. Two important classes of discrete planes are the naive planes and the standard planes, which were mostly studied in the early stage [2,4,24,32]. Later, a new class of graceful planes was introduced in [8] to address the combinatorial issues related to generation of polyhedral meshes and 3D discrete polygons (triangles, for definiteness). 3D graceful lines were subsequently introduced as portions of graceful planes, which ensured that the sides of a 3D triangle are graceful, while the rest (interior) of the triangle remains naive.

The main objective of graceful discretization is to obtain simple analytical description (tunnel-free, in particular) of the basic Euclidean primitives and, on this basis, to create tools for efficient modeling of more sophisticated objects composed by such primitives [8]. Hence, alongside the studies related to naive spheres and standard spheres that are found in the literature of arithmetic geometry, a study on graceful spheres is imminent for a complete understanding of sphere discretization as in the case of plane discretization. With this motivation, we present here for the first time a study on the definition, characterization, and several discrete-geometric issues and outcomes related with graceful spheres. As a prelude, it is worth-mentioning that a graceful sphere in principle is analogous to a graceful plane by its fundamental property. Just like a graceful plane, which is the thinnest discretization of a Euclidean plane satisfying the minimal connectivity of any linear segment on it, a graceful sphere is also the thinnest discretization of a Euclidean sphere with the requisite property that any circular (geodesic) arc on it is a minimally connected set of voxels. The voxel set corresponding to the naive sphere becomes thinnest, and hence contains minimal number of voxels with 2-separating property. Since a graceful sphere is essentially built on a naive sphere with minimum addition of Steiner voxels, its voxel set eventually becomes thinnest and minimal too, and hence, in principle, conforms to the notion of a graceful surface explained in [8]. An introductory example showing a definite advantage of a graceful sphere over a naive sphere is shown in Fig. 1. As evident from this example, the connectivity of an edge (3D geodesic or circular arc) of a Mobius triangle is not guaranteed when defined on a naive sphere, which is however ensured when the edges are taken from the corresponding graceful sphere.

The rest of the paper is organized as follows. In Section 2, we discuss the preliminary ideas, definitions, metrics, and some topological basics related to different classes of discretization in the integer space. In Section 3, we introduce an analytical definition of graceful sphere, derive its related characterization, and explain how it ensures the connectivity of 3D circles and circular arcs, when defined on a graceful sphere in an appropriate topological framework. In Section 4, we establish the relation among naive, standard, and graceful spheres, and discuss different classes of algorithms for construction of Mobius triangles and resultant polygons with necessary connectivity on different types of discrete spherical surfaces. Finally, in Section 5, we draw our concluding notes with further scope and few open problems.

2. Preliminaries

2.1. Basic notions and notations

In this section, we fix some basic notions and notations to be used in the sequel. For more details we refer to [32]. Some other notions will be defined in the subsequent sections.

A *voxel* (also called a 3-cell) is a unit cube determined by the integer grid and fully identified by its center which is a point of $\mathbb{Z}^3$. A discrete (or digital) object is a finite set of voxels. The *supercover* of a set $M \subseteq \mathbb{R}^3$ is the set $S(M)$ of all voxels that are intersected by M.

Two voxels are said to be 0-*adjacent* if they share a vertex (0-cell), 1-*adjacent* if they share an edge (1-cell), and 2-*adjacent* if they share a face (2-cell). Thus, two distinct voxels, $p_1(i_1, j_1, k_1)$ and $p_2(i_2, j_2, k_2)$ are 1-*adjacent* if and only if

[2] also called "analytic discrete geometry".

Please cite this article in press as: R. Biswas, et al., On the polyhedra of graceful spheres and circular geodesics, Discrete Applied Mathematics (2015), http://dx.doi.org/10.1016/j.dam.2015.11.017

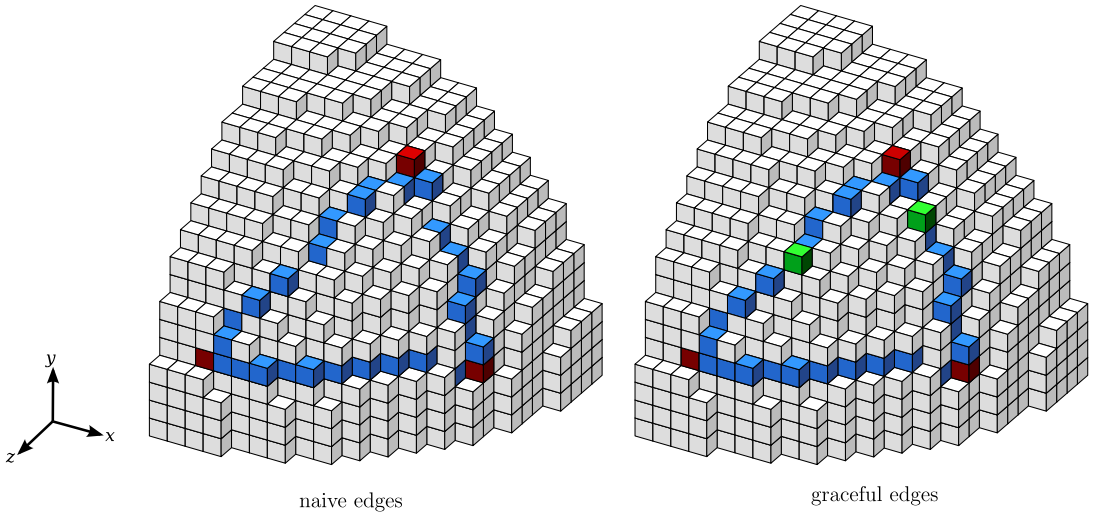

Fig. 1. *Mobius triangles* formed on the 1st c-octant of the *naive sphere* of $r = 15$. Left: *naive edges*. Right: *graceful edges*. Notice that two of the three edges are disconnected when they are naive, whereas all three are minimally connected when they are graceful, as *Steiner voxels* (shown in green) are included. (For interpretation of the references to color in this figure legend, the reader is referred to the web version of this article.)

$|i_1-i_2|+|j_1-j_2|+|k_1-k_2| \leqslant 2$ and $\max\{|i_1-i_2|, |j_1-j_2|, |k_1-k_2|\} = 1$; 2-*adjacent* if and only if $|i_1-i_2|+|j_1-j_2|+|k_1-k_2| = 1$; and 0-*adjacent* if and only if $|i_1-i_2| = |j_1-j_2| = |k_1-k_2| = 1$. Clearly, 0-adjacent (1-adjacent) voxels are not considered as adjacent while considering 1-adjacency (2-adjacency). Note that the 0-, 1-, and 2-adjacencies, as adopted in this paper, correspond respectively to the classical 26-, 18-, and 6-neighborhood notations used in [19].

For $k = 0$, 1, or 2, a *k-path* in a discrete object A links elements through j-facets, where $j \geqslant k$. More precisely, it is a sequence of discrete points from A such that every two consecutive points are k-adjacent. A is called *k-connected* if there is a k-path connecting any two points of A. A *k-component* is a maximal k-connected subset of A.

Let D be a subset of a discrete object A. If $A \setminus D$ is not k-connected, then the set D is said to be *k-separating* in A. Let D be a k-separating digital object in A such that $A \setminus D$ has exactly two k-components. A *k-simple cell* (or *k-simple point*) of D (with respect to A) is a 3-cell c such that $D \setminus \{c\}$ is still k-separating in A. A k-separating digital object in A is *k-minimal* (or *k-irreducible*) if it does not contain any k-simple cell (with respect to A). If a digital object D is not 2-separating in a digital object A, then D has *tunnels*; otherwise, it is *tunnel-free*.

Given a discrete object $A \subseteq \mathbb{Z}^3$, we say that a coordinate plane, say, xy, is functional for A, if for every voxel $v = (x_0, y_0, z_0) \in A$ there is no other voxel in A with the same first two coordinates.

In the considerations that follow, a graceful sphere appears to be a naive sphere to which voxels are added at certain special locations. By analogy to other geometric problems, we will refer to these voxels as *Steiner voxels*.

Let A be a discrete object in $\mathbb{Z}^3$ equipped with a k-adjacency relation ($k \in \{0, 1, 2\}$), and let $G = (V, E)$ be the undirected graph whose vertex set V consists of the centers of voxels in A and edges defined by $e = (u, v) \in E$ iff u and v are k-adjacent in E. Then a *shortest path* between two voxels s and t in A is a sequence of voxels whose centers form a shortest path in G between the vertices corresponding to s and t.

2.2. Metrics and topology

We define *x-distance* and *y-distance* between two (real or integer) points, $p(i, j)$ and $p'(i', j')$, as $d_x(p, p') = |i - i'|$ and $d_y(p, p') = |j - j'|$, respectively. In $\mathbb{R}^3$ or in $\mathbb{Z}^3$, we have also *z-distance*, given by $d_z(p, p') = |k - k'|$, for $p(i, j, k)$ and $p'(i', j', k')$. Using these inter-point distances, we define the respective x-, y-, and z-distances between a point $p(i, j, k)$ and a surface S as follows. Let $d_x(p, S)$ be the x-distance between a point $p(i, j, k)$ and a surface S. If there exists a point $p'(x', y', z')$ in S such that $(y', z') = (j, k)$, then $d_x(p, S) = d_x(p, p')$; otherwise, $d_x(p, S) = \infty$. The other two distances, i.e., $d_y(p, S)$ and $d_z(p, S)$, are defined in a similar way; note that the metric $d_z(p, S)$ is not defined in 2D. An example is shown in Fig. 2.

The above metrics are used to define the *isothetic distance* between two points, or between a point and a curve, or between a point and a surface. Between two points, $p_1(i_1, j_1)$ and $p_2(i_2, j_2)$, the isothetic distance is taken as the *Minkowski norm* [32], given by $d_\infty(p_1, p_2) = \max\{d_x(p_1, p_2), d_y(p_1, p_2)\}$. Between a 2D point $p(i, j)$ and a curve C, it is $d_\perp(p, C) = \min\{d_x(p, C), d_y(p, C)\}$, where $d_x(p, C)$ and $d_y(p, C)$ are defined similar to $d_x(p, S)$ and $d_y(p, S)$ respectively. Between a 3D point $p(i, j, k)$ and a surface S, it is $d_\perp(p, S) = \min\{d_x(p, S), d_y(p, S), d_z(p, S)\}$.

Please cite this article in press as: R. Biswas, et al., On the polyhedra of graceful spheres and circular geodesics, Discrete Applied Mathematics (2015), http://dx.doi.org/10.1016/j.dam.2015.11.017

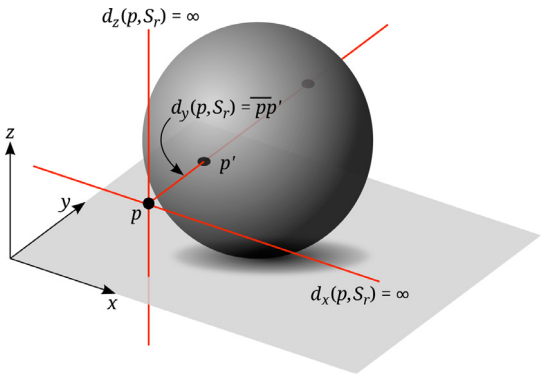

Fig. 2. Isothetic distance of a point p from a real sphere S_r. In this example, $d_x(p, S_r) = d_z(p, S_r) = \infty$, $d_y(p, S_r) = d_y(p, p')$, wherefore $d_\perp(p, S_r) = d_y(p, p') = \overline{pp'}$.

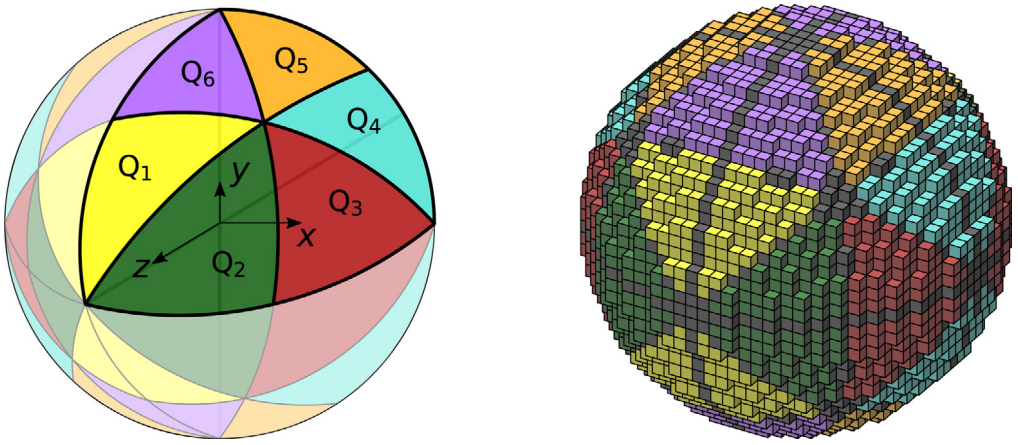

Fig. 3. Quadraginta octants of a real sphere (left) and the voxel set corresponding to its lattice sphere (right), produced by our algorithm, for $r = 15$. A voxel shown in gray belongs to two or more q-octants. (For interpretation of the references to color in this figure legend, the reader is referred to the web version of this article.)

2.3. Discrete sphere representation

A discrete sphere has nine planes of symmetry. These include three coordinate planes, and for each of these three planes, two more planes aligned at $+45°$ and $-45°$ to it. These nine planes of symmetry lead to $2^3 = 8$ *coordinate octants*, which we call *c-octants* for brevity. The three coordinate values of each c-octant can be ordered in $3! = 6$ ways, thereby further dividing the sphere into $8 \times 6 = 48$ *quadraginta octants* [20], or *q-octants* in short. Each c-octant, as well as each q-octant, has a unique relationship among the x-, y-, and z-coordinate values of its constituent points (Fig. 3). This relationship is valid both in $\mathbb{R}^3$ and in $\mathbb{Z}^3$. The c-octants and the q-octants are given specific notations according to these relations, as explained in [6].

By dint of 48-symmetric property, a discrete sphere can be developed from its *prima quadraginta octant*. Hence, for construction of S_r, we can generate only its first q-octant, namely $\mathsf{S}_r^{(1)}$, and reflect it about the planes of symmetry for obtaining the complete set S_r as a 2-minimal set. The set S_r is 1-connected, 2-minimal, and tunnel-free, and also well-voxelized, thereby conforming to the concepts proposed in [19]. The 48-symmetry of sphere can be visualized from Fig. 3.

The c-octants and the q-octants are uniquely represented by 3-tuples; see details in [6]. Each c-octant $\mathbb{C}_i$ is represented by a 3-tuple of signs of coordinate axes, namely $C_i := \left(c_i^{(1)}, c_i^{(2)}, c_i^{(3)}\right)$. For example, $C_1 = (+, +, +)$, $C_2 = (-, +, +)$, and so forth. The 3-tuple for each q-octant $\mathbb{Q}_i$, on the contrary, represents the three signed coordinate axes. In particular, in the 3-tuple $Q_i := \left(q_i^{(1)}, q_i^{(2)}, q_i^{(3)}\right)$ representing $\mathbb{Q}_i$, each element $q_i^{(\cdot)}$ has two variables, namely ω and σ. The variable ω contains a literal (name of the coordinate axis) from $\{\mathtt{x}, \mathtt{y}, \mathtt{z}\}$, and the variable σ contains the sign of the corresponding coordinate. With this representation, we have $Q_1 = (+\mathtt{x}, +\mathtt{y}, +\mathtt{z})$, $Q_2 = (+\mathtt{y}, +\mathtt{x}, +\mathtt{z})$, $Q_3 = (+\mathtt{y}, +\mathtt{z}, +\mathtt{x})$, …, $Q_{24} = (-\mathtt{x}, +\mathtt{z}, -\mathtt{y})$, …, $Q_{48} = (-\mathtt{x}, -\mathtt{z}, -\mathtt{y})$. That is, for Q_{24} as an instance, we have $\omega[q_{48}^{(1)}] = \mathtt{x}$, $\sigma[q_{48}^{(1)}] = \text{`}-\text{'}$, $\omega[q_{48}^{(2)}] = \mathtt{z}$, etc.

Please cite this article in press as: R. Biswas, et al., On the polyhedra of graceful spheres and circular geodesics, Discrete Applied Mathematics (2015), http://dx.doi.org/10.1016/j.dam.2015.11.017

2.4. Naive sphere

Based on the above definitions, a discrete sphere is said to be 2-separating if it does not contain any tunnel, that is, its interior and exterior are not connected by a 2-connected path [19]. A 2-separating discrete sphere is *naive* if and only if it does not contain any simple voxel, that is, removal of any voxel violates its topological property of 2-separableness [19]. Our work is based on the following definition of (discrete) naive sphere.

Definition 1. A *naive sphere* S_r is a 2-minimal (i.e., irreducible and 2-separating) set of voxels having isothetic distance less than $\frac{1}{2}$ from S_r.

Starting from the above definition, a mathematically refined analytical definition of S_r, as given in [6], is as follows.

Theorem 1 (*Naive Sphere*)**.** *The naive sphere of radius r is given by*

$$\mathsf{S}_r = \left\{ \begin{array}{c} (i,j,k) \in \mathbb{Z}^3 : r^2 - \max\{|i|,|j|,|k|\} \leqslant i^2+j^2+k^2 < r^2 + \max\{|i|,|j|,|k|\} \\ \wedge \Big(\big(i^2+j^2+k^2 \neq r^2 + \max\{|i|,|j|,|k|\} - 1\big) \\ \vee (\mathrm{mid}\{|i|,|j|,|k|\} \neq \max\{|i|,|j|,|k|\}) \Big) \end{array} \right\}. \tag{1}$$

It gives a useful directive to an integer algorithm. Further, the mathematical interpretation of a naive sphere by the above theorem provides an interesting property of a geodesic path connecting any source–destination pair$(s,t) \in \mathsf{S}_r \times \mathsf{S}_r$. If $P_r(s,t)$ denotes the real geodesic plane passing through s and t (and the center of S_r), and if $\mathrm{I}_r(s,t)$ denotes the set of voxels of S_r that are intersected by $P_r(s,t)$, then there always exists a 1-connected cycle in $\mathrm{I}_r(s,t)$. The set $\mathrm{I}_r(s,t)$ admits the characterization that all its voxels lie within an isothetic distance of $\frac{3}{2}$ from $P_r(s,t)$. Subsequently, the discrete spherical geodesic path $\boldsymbol{\pi}_r(s,t)$ becomes a subset of $\mathrm{I}_r(s,t)$, and is efficiently obtained just from r, s, t based on Theorem 1, without considering the entire voxel set, S_r. The time complexity thus becomes optimal, that is, linear in the geodesic path length from s to t.

3. Graceful sphere and geodesic paths

As mentioned in Section 2.4, a (discrete) spherical geodesic path on the naive sphere may contain voxels with isothetic distance as high as $\frac{3}{2}$ from the real geodesic plane. This, in fact, makes the geodesic path somewhat jagged. The jaggedness can be reduced if we ensure that the geodesic path is digitally circular, which happens if, for a given source–destination pair (s,t) from a naive sphere of radius r, the path is constituted by voxels intersected by some real 3D circular arc. However, this is not always possible if the path is made of voxels only from the naive sphere. Similar situation also arises in naive planes, and it is tackled quite efficiently when a discrete plane is considered to be *graceful*. The following section gives an overview of this concept in the context of our work.

3.1. Graceful plane

Detailed study and analysis related to graceful planes may be seen in [7,13,8–10]. Following is a comprehensive definition of graceful plane adopted from [8].

Definition 2 (*Graceful Plane*)**.** A graceful plane is the thinnest possible discrete plane for which, in the framework of generation scheme, Euclidean primitives like lines, segments, and triangles (as well as arbitrary polygons) are always connected sets of voxels.

The notion of *gracefulness* used in discrete planes is also relevant and has a significant theoretical importance to many issues related to discrete spheres. To start with, we first make a brief review on the merits of gracefulness in case of discrete planes.

Let P be a 3D real plane, P and $\mathscr{P}$ be its corresponding naive and graceful planes, and let the functional plane be F. Let s and t be two voxels on P. Let s' and t' be the projections of s and t on F. Let $L(s',t')$ be the 2D digital straight segment (DSS) joining s' and t' on F. As there is a one-to-one correspondence between voxels on P and pixels on F, we will get a set of voxels on P corresponding to the pixels of $L(s',t')$. This set may not be connected due to presence of one or more *jumps* [8]. Each jump is created by a pair of disconnected voxels, as illustrated in Fig. 4(a). This problem is solved in $\mathscr{P}$ by inserting a *Steiner voxel* in between the two voxels forming a jump in P so that those two voxels become 0-connected in $\mathscr{P}$. A *tandem* is thus formed by the Steiner voxel and one of the jump voxels, so that they are 2-adjacent to each other (Fig. 4(b)). To ensure that $\mathscr{P}$ is a subset of the supercover $\boldsymbol{P}$ of the corresponding real plane, each Steiner voxel is chosen only if it has an intersection with the real plane.

Please cite this article in press as: R. Biswas, et al., On the polyhedra of graceful spheres and circular geodesics, Discrete Applied Mathematics (2015), http://dx.doi.org/10.1016/j.dam.2015.11.017

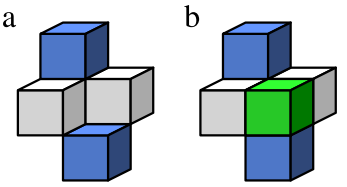

Fig. 4. Example of adding a Steiner voxel to a naive surface to make it graceful. (a) A *jump* (blue voxel pair) on a naive surface (plane or sphere, as the case may be). All the four (two white and two blue) voxels belong to the naive surface. (b) A *tandem* constituted by the lower voxel of the jump and a *Steiner voxel* (green) belonging to the graceful surface. (For interpretation of the references to color in this figure legend, the reader is referred to the web version of this article.)

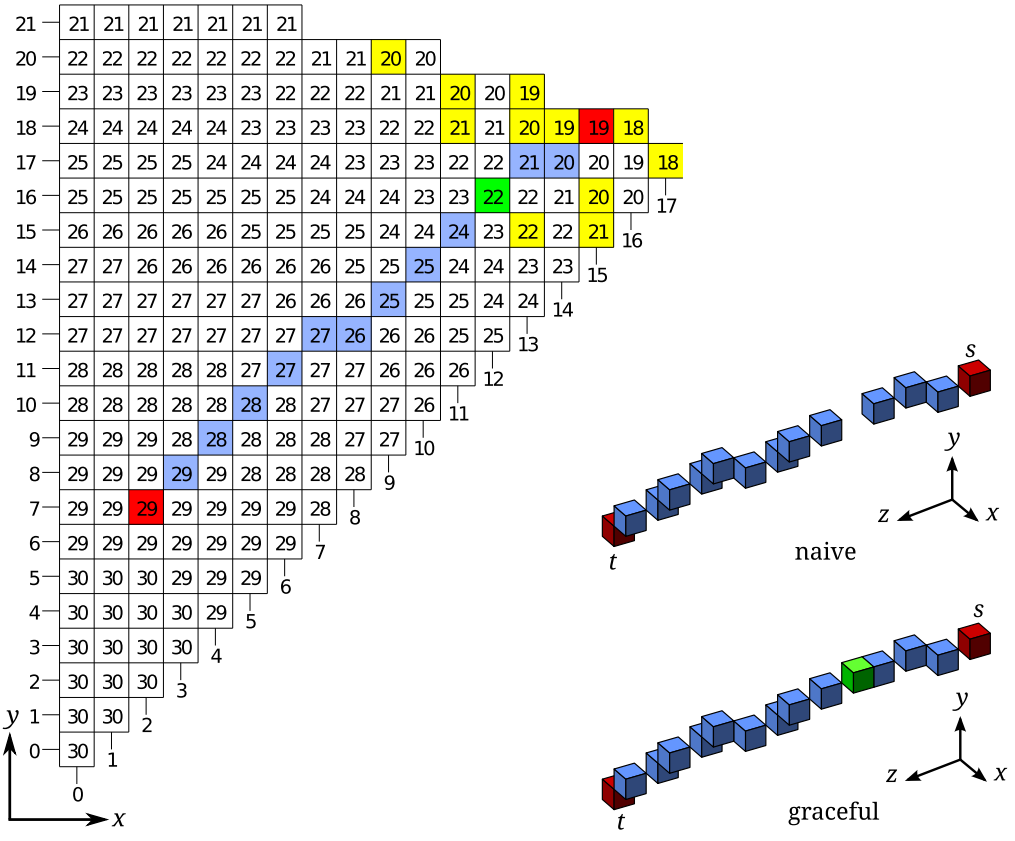

Fig. 5. Projection of $S_r^{(1)}$ for $r = 30$ on its functional (i.e., xy) plane. Positions of all possible Steiner voxels are shown in yellow. For $s = (15, 18, 19)$, $t = (2, 7, 29)$, there is a gap in the circular segment defined on the naive sphere. The Steiner voxel (green) forms a tandem with a voxel of the circular segment on the naive sphere, and hence forms a 0-connected circular segment on the graceful sphere. Notice that the tandem configuration is same as that found in a naive discrete plane shown in Fig. 4. (For interpretation of the references to color in this figure legend, the reader is referred to the web version of this article.)

3.2. Graceful sphere

The topological enhancement of a naive to a graceful sphere has a close resemblance with that from a naive to a graceful plane. More precisely, the topological difference in either case is caused by the presence of jumps, which occur in multitude. Characterization and fixing of jumps by corresponding tandems provides certain theoretical advantages in case of the graceful surface, be it a plane or be it a sphere. Such a strong notional commonality between a graceful plane and a graceful sphere naturally leads us to introduce the following definition of graceful sphere.

Definition 3 (*Graceful Sphere*)**.** A graceful sphere is the thinnest possible discrete sphere for which, in the framework of generation scheme, Euclidean primitives like geodesic paths, geodesic circles, and Mobius/spherical triangles (as well as arbitrary spherical polygons) are always well-connected sets of voxels.

Fig. 5 shows a detailed illustration of a jump and its tandem that are found and fixed to construct a circular segment on a naive sphere. Notice that they are similar in configuration to those arising in case of a naive plane. However, there is a marked

Please cite this article in press as: R. Biswas, et al., On the polyhedra of graceful spheres and circular geodesics, Discrete Applied Mathematics (2015), http://dx.doi.org/10.1016/j.dam.2015.11.017

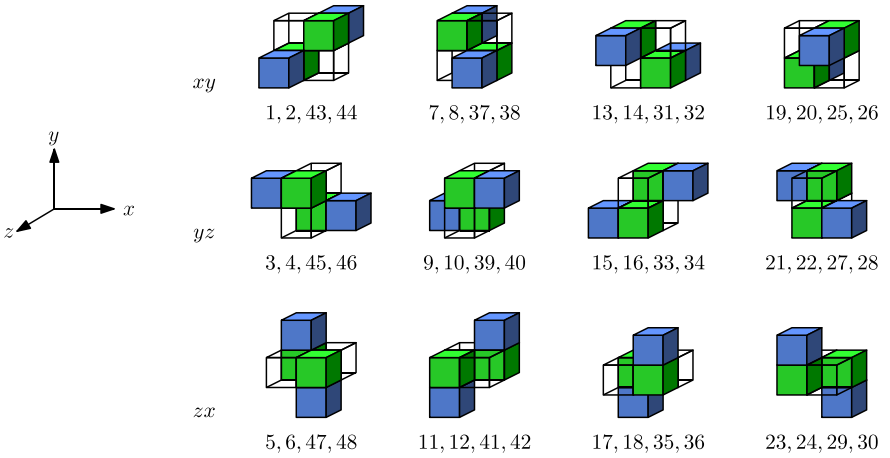

Fig. 6. Tandem configurations appearing on 48 q-octants, as shown below the respective configurations. Configurations with the same functional plane are shown in a row. The two voxels comprising a jump are shown in blue, and the other two voxels of naive sphere are shown hollow. The two voxels shown in green are Steiner voxels, and a graceful geodesic path would include at most one of them. (For interpretation of the references to color in this figure legend, the reader is referred to the web version of this article.)

difference between the set of configurations corresponding to a plane and that corresponding to a sphere. This difference arises due to the fact that a naive plane always has a fixed functional plane, while a naive sphere has all three coordinate planes as functional planes. In particular, a particular q-octant has a specific functional plane, owing to 48-symmetry of naive sphere, which is explained below.

Functional planes. Let $\mathsf{S}_r^{(q)}$, where $q = 1, 2, \ldots, 48$, be the qth q-octant of any naive sphere of radius r. Then its functional plane is the *xy*-, *yz*-, or *zx*-plane, depending on whether the value of q mod 6 belongs to $\{1, 2\}$, $\{3, 4\}$, or $\{5, 0\}$, respectively. Hence, depending on the q-octant that a Steiner voxel belongs to, we get the functional plane so that we can apply the tandem configuration used for a graceful plane with the same functional plane. This is possible due to the fact that $\mathsf{S}_r^{(q)}$ has one-to-one correspondence with its projection on its functional plane. For a group of four q-octants, we get an identical tandem configuration. As a result, the total number of tandem configurations is 12, since the 48 q-octants of a naive sphere follow an octahedral symmetry. The different symmetric variants of the tandem configurations appearing in all the q-octants of a sphere are shown in Fig. 6. It is also to be noted that only one particular variant of tandem configuration appears in a particular q-octant. A Steiner voxel can be put either outside the naive sphere, or inside, in between the jump voxels to connect them, according to its intersection with the real sphere. The Steiner voxels belonging to q-octants of a graceful sphere with different functional planes are shown in Fig. 7, with a coloring based on their functional planes.

Steiner voxels. As each q-octant of a naive sphere has a particular functional plane, it always has a particular tandem configuration, which provides a simple solution to put in any Steiner voxel in that q-octant. We have the following lemma on the Steiner voxels for the 1st q-octant of $\mathcal{S}_r$, which follows from the fact that the functional plane of $\mathsf{S}_r^{(1)}$ is *xy*-plane.

Lemma 1. *(i, j, k) is a Steiner voxel in $\mathbb{Q}_1$ if and only if $i \leqslant j \leqslant k$ and the four voxels $(i+\Delta, j, k)$, $(i, j+\Delta, k)$, $(i, j, k+\Delta)$, $(i+\Delta, j+\Delta, k-\Delta)$ belong to S_r for $\Delta = -1$ or 1.*

The above lemma leads to the following theorem that formulates whether any voxel is a Steiner voxel, irrespective of its location in terms of q-octants.

Theorem 2. *The set of all Steiner voxels of $\mathcal{S}_r$ is given by*

$$T_r = \Big\{(i,j,k) : \big(\{(i'+\Delta, j', k'), (i', j'+\Delta, k'), (i', j', k'+\Delta), (i'+\Delta, j'+\Delta, k'-\Delta)\} \subset \mathsf{S}_r\big) \wedge \big(i' = \min(|i|, |j|, |k|)\big) \wedge \big(j' = \mathrm{mid}(|i|, |j|, |k|)\big) \wedge \big(k' = \max(|i|, |j|, |k|)\big) \wedge \big(\Delta \in \{-1, 1\}\big)\Big\}.$$

Proof. It is based on the fact that (i, j, k) is a Steiner voxel of $\mathcal{S}_r$ if and only if (i', j', k') is a Steiner voxel in $\mathbb{Q}_1$, with i', j', k' denoting the respective minimum, median (mid), and maximum element in $\{|i|, |j|, |k|\}$. This follows from Lemma 1 and the 48-symmetry of naive sphere explicated in Theorem 1. □

Addition of Steiner voxels converts a naive sphere to its corresponding graceful sphere. This gives us an analytical characterization of graceful sphere based on the fact that it is the union of naive sphere and the set of requisite Steiner voxels. Hence, the graceful sphere of radius r is given by

$$\mathcal{S}_r = \big\{(i, j, k) : (i, j, k) \in \mathsf{S}_r \vee (i, j, k) \in T_r\big\}. \tag{2}$$

Please cite this article in press as: R. Biswas, et al., On the polyhedra of graceful spheres and circular geodesics, Discrete Applied Mathematics (2015), http://dx.doi.org/10.1016/j.dam.2015.11.017

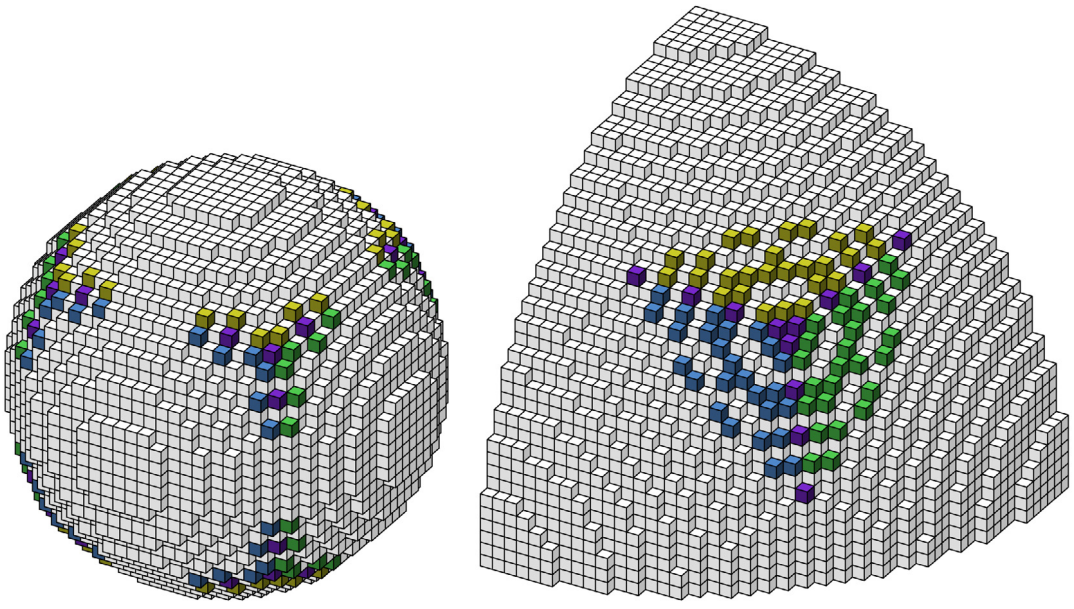

Fig. 7. A graceful sphere for $r = 15$ (left) and only 1st c-octant of graceful sphere for $r = 30$ (right). Voxels comprising the naive sphere are shown in white, and the Steiner voxels in color. Yellow, green, and blue are for three different functional planes, and violet indicates two or more functional planes for the same Steiner voxel. (For interpretation of the references to color in this figure legend, the reader is referred to the web version of this article.)

We conclude this section with the following observation. It is well-known that on an unbounded graceful plane the tandems form an infinite lattice. With a reference to Fig. 7, on a graceful sphere (which is a bounded isothetic polyhedron) the tandems locations feature a lattice of clusters, the latter being of somewhat circular structure.

3.3. Graceful geodesic path

A real *geodesic path* on a real sphere S_r of radius r is defined between two points p and q lying on S_r. The path always lies along the intersection circle of S_r and the *geodesic plane* passing through p, q, and the center ($o = (0, 0, 0)$, w.l.o.g.) of S_r. In the discrete space, it is defined in a similar way. Let $\mathrm{I}_r(s, t)$ be the set comprising the voxels of S_r that are intersected by $P_r(s, t)$. Then we have the following definition of naive geodesic path on S_r.

Definition 4 (*Naive Geodesic, See [6]*)**.** A naive geodesic path $\boldsymbol{\pi}_r(s, t)$ from $s \in \mathsf{S}_r$ to $t \in \mathsf{S}_r$ is a l-connected ($l = 0, 1$) shortest path in $\mathrm{I}_r(s, t)$ from s to t.

Generation of a naive geodesic path is done in [6] from $\mathrm{I}_r(s, t)$ by an optimal-time algorithm, called DSGP, based on prioritized-BFS. An example of $\mathrm{I}_r(s, t)$ is shown in Fig. 8. Although the path from s to t produced by the algorithm DSGP always consists of the smallest set of voxels from $\mathrm{I}_r(s, t)$, it may not be digitally circular. This is illustrated in Fig. 9. On the contrary, if the path is defined on a graceful sphere, then it is not only one of the shortest paths from s to t but also digitally circular in the 3D discrete space. We introduce the following definition for this.

Definition 5 (*Graceful Geodesic*)**.** A *graceful geodesic path* $\tilde{\boldsymbol{\pi}}_r(s, t)$ from $s \in \mathsf{S}_r$ to $t \in \mathsf{S}_r$ is a 0-connected digitally circular path comprising voxels intersected by S_r.

One main reason of finding graceful geodesic paths is to ensure the connectivity of 3D circular segments on a discrete spherical surface. As shown in [6], the voxels of S_r intersected by $P_r(s, t)$ (i.e., $\mathrm{I}_r(s, t)$) always form a 1-connected set. This property can be used to derive a stronger result, as stated shortly in Theorem 3. For this, we define the following terms.

Real geodesic circle, $C_r(s, t)$, given by the intersection of S_r with $P_r(s, t)$.

Elliptical projection (e.g., $E_r^{xy}(s, t)$ on xy-plane) obtained by projecting $C_r(s, t)$ on a coordinate plane.

Closed naive geodesic path, $\boldsymbol{\Pi}_r(s, t)$, obtained by concatenating $\boldsymbol{\pi}_r(s, t)$ with $\boldsymbol{\pi}_r(t, s)$.

Theorem 3. *Projection of $\boldsymbol{\Pi}_r(s, t)$ on any coordinate plane is always 0-connected and contains the digitization of the elliptical projection of $C_r(s, t)$ on that plane.*

Please cite this article in press as: R. Biswas, et al., On the polyhedra of graceful spheres and circular geodesics, Discrete Applied Mathematics (2015), http://dx.doi.org/10.1016/j.dam.2015.11.017

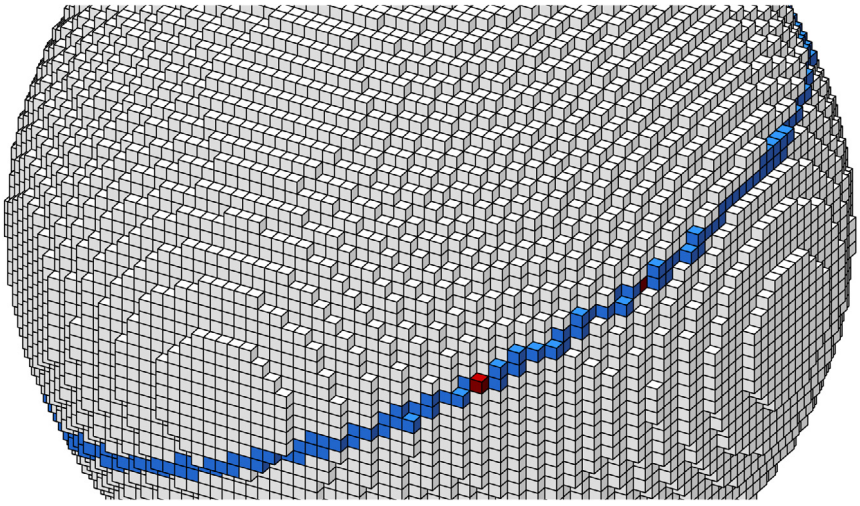

Fig. 8. An intersection set on the naive sphere of radius 30.

Proof. Intersection of S_r with $P_r(s, t)$ produces the 3D real circle $C_r(s, t)$. Projection of $C_r(s, t)$ on xy-, yz-, and zx-planes gives us three ellipses, namely $E_r^{xy}(s, t)$, $E_r^{yz}(s, t)$, and $E_r^{zx}(s, t)$, respectively. One of these ellipses may degenerate to a line segment, e.g., when $s = (0, 0, r)$. Consider, w.l.o.g., the ellipse $E_r^{xy}(s, t)$. As shown in [6], the set $\mathrm{I}_r(s, t)$, which is the intersection of S_r with the supercover of $P_r(s, t)$, is a 1-connected subset of the supercover of $C_r(s, t)$. From $\mathrm{I}_r(s, t)$, we get $\boldsymbol{\Pi}_r(s, t)$ as a 0-connected set. Since the projection of a 0-connected 3D set on any coordinate plane is always a 0-connected set of pixels, the projected set of $\boldsymbol{\Pi}_r(s, t)$ on xy-plane will be 0-connected and a subset of the supercover of $E_r^{xy}(s, t)$. Similar arguments hold for projections of $\boldsymbol{\Pi}_r(s, t)$ on the other two coordinate planes. □

Theorem 3 just indicates that the projection of $\boldsymbol{\Pi}_r(s, t)$ is 0-connected, but it does not tell explicitly about the nature of its connectivity; in fact, it may not be irreducible owing to the presence of one or more simple pixels. In particular, we have the following theorem.

Theorem 4. *Piecewise projections of $\boldsymbol{\Pi}_r(s, t)$ on its respective functional planes may contain simple pixels, and removal of a voxel from $\boldsymbol{\Pi}_r(s, t)$ corresponding to any of these simple pixels makes it disconnected.*

Proof. W.l.o.g., consider a sub-path of $\boldsymbol{\Pi}_r(s, t)$ in some q-octant so that it is functional on xy-plane. As per the construction of a naive sphere (Definition 1), the sub-path is a sequence of voxels with monotonically non-increasing (or non-decreasing) values of z-coordinate, and the z-values of two consecutive voxels in this sequence differ by at most unity. By Theorem 3, the projection of this sub-path on xy-plane is a 0-connected sequence of pixels. Hence, if there are two 0-adjacent pixels a' and b' in this projection so that their corresponding voxels a and b in the sub-path differ by 2 in their z-values, then a and b form a jump and are 0-connected in the sub-path through some other voxel c. Hence, the projection c' of c on xy-plane becomes a simple pixel. This implies that removal of c' from the projection makes it irreducible, but removal of the corresponding voxel c disconnects a and b in the sub-path. Hence the proof. □

As shown in Fig. 9, the pixels with $z = 24$ and $z = 22$ correspond to a pair of voxels comprising a jump, and the pixel with $z = 23$ is a simple pixel. Removal of the voxel corresponding to this simple pixel produces a disconnected path, as shown earlier in Fig. 5. In order to restore the connectivity of the disconnected path with the guarantee of its digital circularity, Steiner voxels are necessary and sufficient. We have the following theorem.

Theorem 5. *Inclusion of Steiner voxels in a disconnected naive geodesic path produces a digitally circular path whose piecewise projection on the corresponding functional planes produces irreducible* 0*-connected discrete elliptical segments.*

Proof. As in Theorem 4, consider w.l.o.g. a sub-path of $\boldsymbol{\pi}_r(s, t)$ in some q-octant with xy-plane as its functional plane. Take its projection on xy-plane, and delete the simple pixels from this projection so that it is minimal and 0-connected. By Theorem 4, the deletion of corresponding voxels from the sub-path makes $\boldsymbol{\pi}_r(s, t)$ disconnected due to formation of jumps. If a Steiner voxel is inserted to connect the two voxels forming each jump, then a tandem is formed with respect to xy-plane and hence no simple pixel creeps in. This keeps the projection of the sub-path unaltered, i.e., minimal and 0-connected. □

An illustration of Theorem 5 is given in Fig. 10. These results are subsequently used to design the algorithm for construction of graceful geodesics, as explained next.

Please cite this article in press as: R. Biswas, et al., On the polyhedra of graceful spheres and circular geodesics, Discrete Applied Mathematics (2015), http://dx.doi.org/10.1016/j.dam.2015.11.017

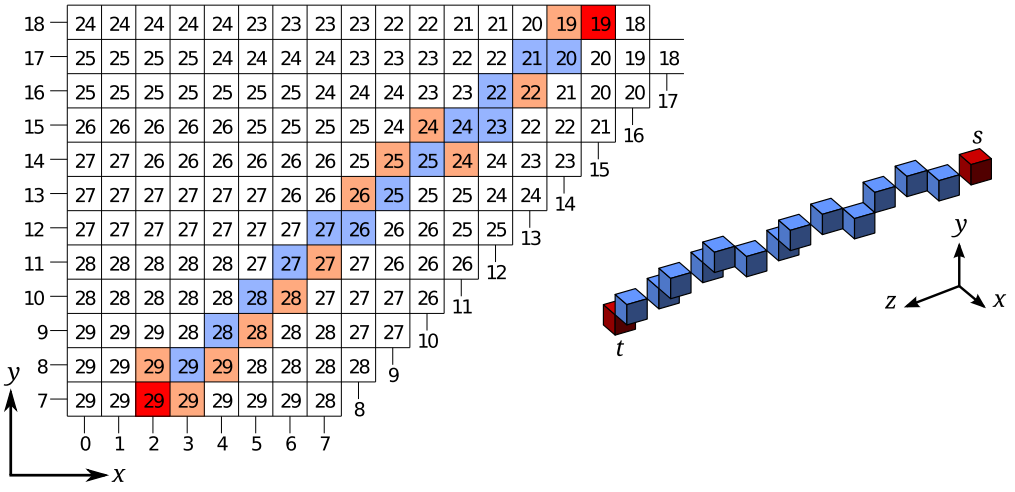

Fig. 9. A naive geodesic path, which is not digitally circular, since the pixel with $z = 23$ is *simple*. The s–t pair and radius r are as in Fig. 5. The pixel pair with $z = 24, 22$ corresponds to a jump voxel pair (Fig. 5).

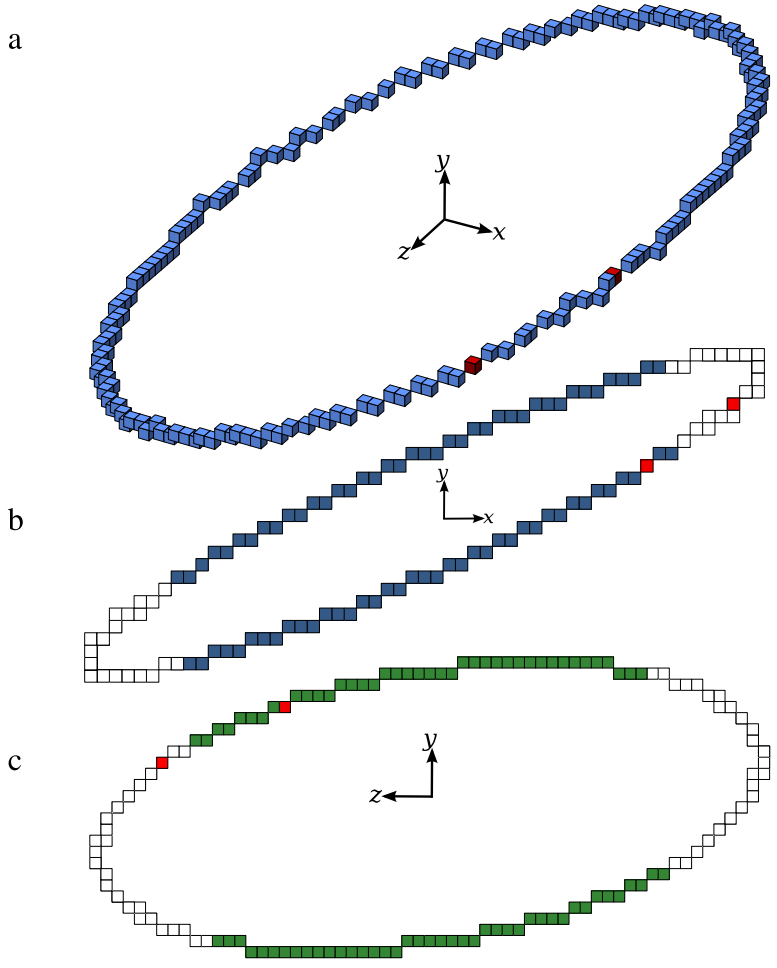

Fig. 10. (a) The closed graceful path $\boldsymbol{\Pi}_r(s, t)$ obtained from the intersection set $\mathrm{I}_r(s, t)$ shown in Fig. 8. (b) and (c) Projections of the segments of the path lying in different q-octants, taken along the corresponding functional (b: xy- and c: yz-) planes. In (b), the red pixel in the blue segment corresponds to s, and the other red one in the white segment corresponds to t. In (c), the red one inside white corresponds to s, and the other red inside green to t. (For interpretation of the references to color in this figure legend, the reader is referred to the web version of this article.)

Please cite this article in press as: R. Biswas, et al., On the polyhedra of graceful spheres and circular geodesics, Discrete Applied Mathematics (2015), http://dx.doi.org/10.1016/j.dam.2015.11.017

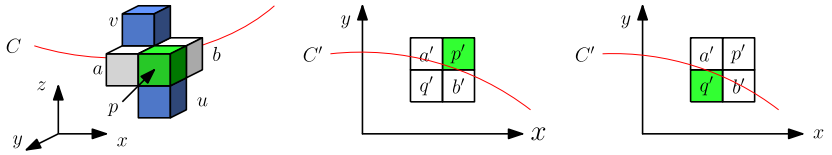

Fig. 11. Illustration of Theorem 6.

3.4. Algorithm for graceful paths

Based on the properties discussed in Section 3.3, we have first designed the algorithm for construction of a graceful geodesic path $\tilde{\boldsymbol{\pi}}_r(s,t)$ that starts from $s \in \mathsf{S}_r$ and ends at $t \in \mathsf{S}_r$. The input to this algorithm comprises s, t, and the radius r. The steps are as follows.

1. Generate a 0-connected naive geodesic path $\boldsymbol{\pi}_r(s,t)$. For this, apply the algorithm DSGP of [6] to get a 1-connected naive geodesic path first, and then do a simple mapping from 1-connections to 0-connections to produce the 0-connected naive geodesic path as its subset.
2. Traverse the path $\boldsymbol{\pi}_r(s,t)$ starting from s and project each voxel in the sequence to its functional plane based on the q-octant it belongs to. It gives one or more connected segments of pixels on the coordinate planes (Theorem 3).
3. For each connected segment on a coordinate plane, find the simple pixels (Theorem 4). Replace the voxel in $\boldsymbol{\pi}_r(s,t)$ corresponding to each simple pixel with the requisite Steiner voxel (Theorem 5).

For construction of a 0-connected 3D discrete circle passing through $s \in \mathsf{S}_r$ and $t \in \mathsf{S}_r$, with the constraint that each of its voxels is intersected by both S_r and $P_r(s,t)$, we first generate $\boldsymbol{\Pi}_r(s,t)$ from $\mathrm{I}_r(s,t)$ by starting the prioritized-BFS from s, passing through t, and ending the traversal also at s, instead of ending at t as in the case of $\boldsymbol{\pi}_r(s,t)$ generation. After getting $\boldsymbol{\Pi}_r(s,t)$, we can simply follow the same steps, as in the case of $\tilde{\boldsymbol{\pi}}_r(s,t)$ generation, to get the 0-connected 3D discrete circle passing through s and t. Fig. 10 shows a result.

4. Naive, standard, and graceful spheres

From the principle of construction of a graceful plane, we can prove that $\mathsf{P} \subseteq \mathscr{P} \subseteq \boldsymbol{P}$, where P, $\mathscr{P}$, and $\boldsymbol{P}$ denote the naive, the graceful, and the standard plane, respectively. An analogous result holds for naive, graceful, and standard spheres also, as stated in the following theorem.

Theorem 6. *$\mathsf{S}_r \subseteq \mathscr{S}_r \subseteq \boldsymbol{S}_r$, where $\mathscr{S}_r$ and $\boldsymbol{S}_r$ denote the respective graceful sphere and the standard sphere corresponding to the naive sphere S_r.*

Proof. By Eq. (2), $\mathsf{S}_r \subseteq \mathscr{S}_r$. So, to prove $\mathscr{S}_r \subseteq \boldsymbol{S}_r$, let p be any Steiner voxel of $\mathscr{S}_r$, as illustrated in Fig. 11. W.l.o.g., let $p(i,j,k)$ lie in $\mathbb{Q}_1$. Let (u,v) define the jump corresponding to p, and let a and b be the other two 2-adjacent voxels of p in S_r. Let $q = (i-1, j-1, k)$. Consider the projections of a, b, p, q on the functional (i.e., xy-) plane, and let them be denoted by a', b', p', q', respectively. Now observe the following. Since a and b are intersected by S_r, there exists some real circle C on S_r, such that the following conditions hold:

1. C is parallel to xy-plane;
2. z-coordinate of C lies between $k - \frac{1}{2}$ and $k + \frac{1}{2}$;
3. projection C' (a circle) of C on the functional plane intersects the pixels (unit squares) a' and b'.

Clearly, the circle C' also intersects p' or q'. W.l.o.g., let C' also intersect p'. Equivalently, C intersects p. As C lies on S_r, it follows that p gets intersected by S_r. Thus, p belongs to $\boldsymbol{S}_r$, whence the proof. □

4.1. Algorithms for Mobius triangles

As explained in [8], graceful planes can be used for modeling of Euclidean primitives and generation of discrete (planar) triangular meshes. For this, 3D discrete triangles are generated based on the 2D triangles obtained by joining the projections of the vertices of the 3D triangles on their respective functional planes. It results to connected and tunnel-free 3D discrete triangles for different methods. In this section, we show how the idea can be extended for discretization of Mobius triangles defined on a spherical surface. We first discuss below a discretization method that results to a connected and tunnel-free Mobius triangle when discretized on a graceful sphere, given that the vertices of the triangle belong to the corresponding naive sphere.

Please cite this article in press as: R. Biswas, et al., On the polyhedra of graceful spheres and circular geodesics, Discrete Applied Mathematics (2015), http://dx.doi.org/10.1016/j.dam.2015.11.017

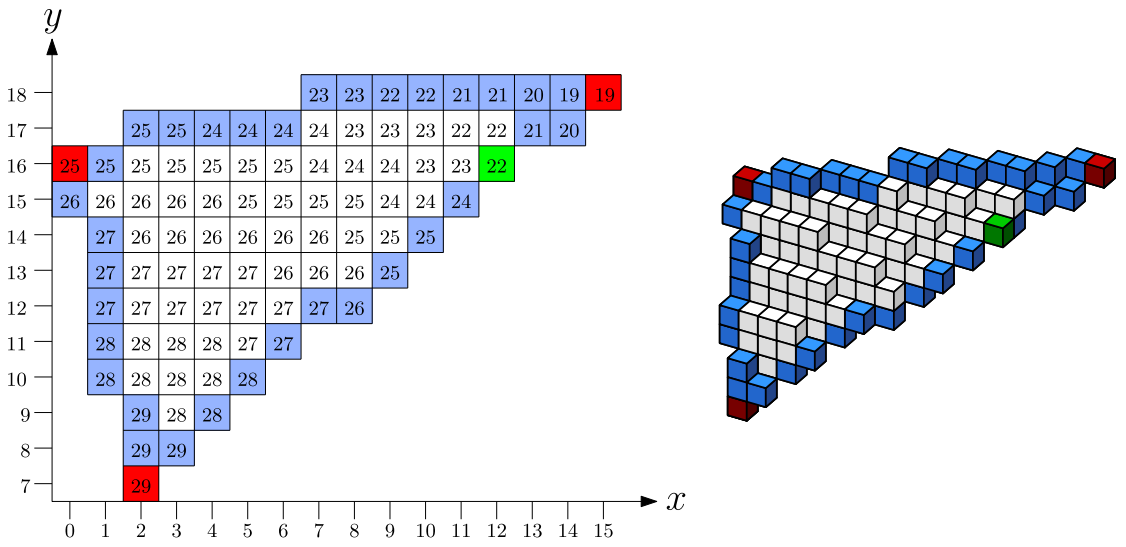

Fig. 12. Construction of a Mobius triangle by GN-method using the projection map.

Graceful sphere method (GG-method).

1. The three sides of the Mobius triangle *abc* are approximated through the corresponding graceful paths (Section 3.4).
2. While computing each graceful side, the q-octants intersected by it are inserted in a list L_1. To do this, for example, for *ab*, the set $\mathrm{I}_r(a, b)$ is used. See [6] for an elaborate discussion.
3. From the list L_1 of q-octants intersected by the three sides of *abc*, each other q-octant that belongs completely to *abc* and is bounded by the q-octants of L_1, is obtained and inserted in another list, L_2. This is done based on the adjacency relation of the q-octants, available from the 3-tuple Q_i corresponding to each q-octant $\mathbb{Q}_i$, as mentioned in Section 2.
4. Each q-octant in L_2 is approximated by its graceful Mobius triangle based on its projection on its functional plane (Section 3.2) and its corresponding equations in Theorems 1 and 2.
5. For each q-octant in L_1, its part belonging to the Mobius triangle is obtained by the projection of the sides of the part on the corresponding functional plane, bounding the projection of the q-octant accordingly, and then doing the inverse mapping as in the previous step.

The above method can be redesigned to the following method to obtain a discrete Mobius triangle with thinner interior.

Graceful sides, Naive Interior method (GN-method).

1. The sides of the Mobius triangle are approximated through the corresponding graceful paths.
2. The interior of the triangle is approximated through the naive spherical parts of the relevant q-octants, with similar steps as in GG-method.

An illustration of GN-method is shown in Fig. 12. It has been shown in [6] that the discrete sphere produced by Theorem 1 is naive and 2-separating, i.e., tunnel-free. Hence, by construction of the graceful sides of the discrete Mobius triangle, its interior becomes disconnected with the rest of the naive sphere. With this, we conclude that the discrete Mobius triangle obtained through the GN-method is connected and tunnel-free.

Another method to obtain a connected and tunnel-free triangular approximation of a spherical surface can be through the standard discretization of the sides of the triangle, as shown below.

Standard sides, Naive Interior method (SN-method).

1. The sides of the Mobius triangle are approximated through the corresponding 2-connected paths lying in the intersection of the standard sphere $\boldsymbol{S}_r$ with the real geodesic plane $P_r(s, t)$.
2. The interior of the triangle is approximated as in GN-method.

Since a standard sphere is 0-separating, its intersection with the real geodesic plane is always 2-connected. Hence, it is ensured that the sides of the Mobius triangle are 2-connected paths. This, in turn, makes the interior of the Mobius triangle 0-separating from the exterior portion of the corresponding naive sphere. A comparison among the Mobius triangles formed by different methods is shown in Fig. 13.

5. Concluding notes

We have proposed a new class of discrete spheres that can be more effective in different discrete-geometric modeling applications. We call these spheres as graceful, as they have a high degree of similitude with the class of graceful planes.

Please cite this article in press as: R. Biswas, et al., On the polyhedra of graceful spheres and circular geodesics, Discrete Applied Mathematics (2015), http://dx.doi.org/10.1016/j.dam.2015.11.017

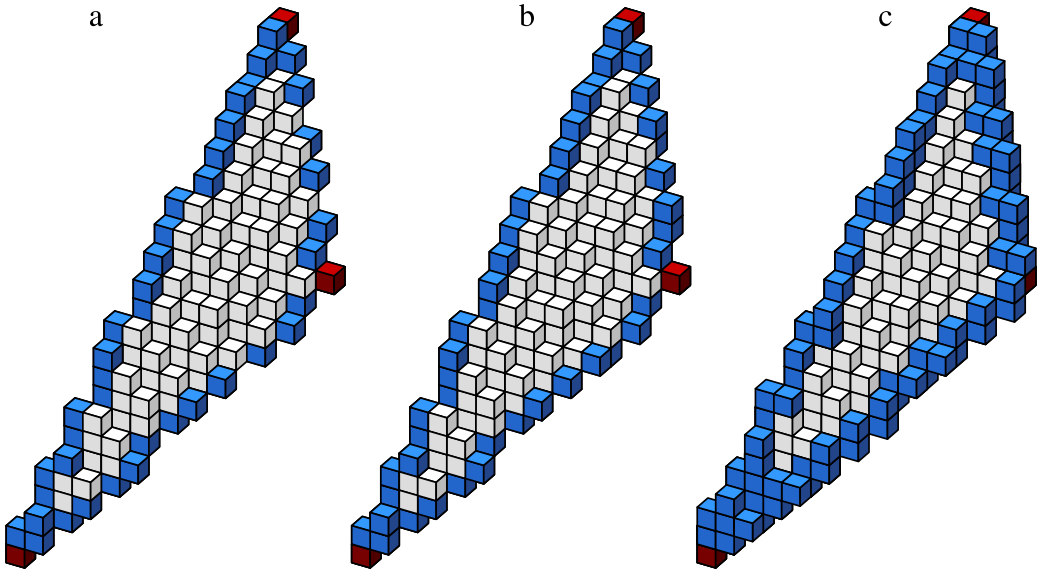

Fig. 13. Comparison among different types of Mobius triangle. For each type in this example, the vertices (shown in red) are (7, 2, 29), (12, 24, 13), (18, 15, 19) and belong to the naive sphere of radius 30; the interior of the triangle is a subset of the naive sphere, and its sides are (a) naive, (b) graceful, (c) standard. (For interpretation of the references to color in this figure legend, the reader is referred to the web version of this article.)

The inherent structure of a graceful sphere makes it "sandwiched" between the corresponding naive and standard spheres, and hence it acquires several useful characteristics. One such characteristic is that discrete geodesic circles and circular arcs with definite connectivity can be constructed on these spheres using a suitable algorithm of geodesic path finding. The idea can be extended to draw Mobius triangles on them, which would be optimally thin, well-connected, and tunnel-free.

We have shown how q-octants play a significant role for exercising the strength of functional planes in solving the sphere-related problems through their 2D projections and inverse maps. The similitude of discrete spheres with discrete planes is established through this, which provides an insight to solve similar approximation problems based on appropriate functional planes in case of other geometric primitives, such as ellipsoids, cones, and cylinders.

Our study has widened the scope of new discretization methodology for spheres. As discussed recently in [12], discretization based on a chosen value of connected distance leads to different *offset models* of a Euclidean primitive. In our work, although we have considered isothetic distance for modeling a discrete sphere, a different distance metric may result to well-formed offset spheres, which may be sandwiched between the corresponding graceful and standard spheres and may be jump-free. Thus, geodesic circles and Mobius triangles can be constructed on them with desired connectivity and tunnel-freeness. Exploring this direction of research is seen as an important future task.

References

[1] E. Andres, Discrete circles, rings and spheres, Comput. Graph. 18 (5) (1994) 695–706.
[2] E. Andres, R. Acharya, C. Sibata, Discrete analytical hyperplanes, Graph. Models Image Process. 59 (5) (1997) 302–309.
[3] E. Andres, M. Jacob, The discrete analytical hyperspheres, IEEE Trans. Vis. Comput. Graphics 3 (1) (1997) 75–86.
[4] E. Andres, M.-A. Jacob, The discrete analytical hyperspheres, IEEE Trans. Vis. Comput. Graphics 3 (1) (1997) 75–86.
[5] A. Balog, I. Bárány, On the convex hull of the integer points in a disc, in: Proc. 7th Annual Symposium on Computational Geometry, SoCG 1991, 1991, pp. 162–165.
[6] R. Biswas, P. Bhowmick, On finding spherical geodesic paths and circles in $\mathbb{Z}^3$, in: Proceedings of the 18th International Conference on Discrete Geometry for Computer Imagery, 2014, pp. 396–409.
[7] V.E. Brimkov, R.P. Barneva, Graceful planes and thin tunnel-free meshes, in: Discrete Geometry for Computer Imagery, in: Lecture Notes in Computer Science, vol. 1568, Springer, Berlin, Heidelberg, 1999, pp. 53–64.
[8] V.E. Brimkov, R.P. Barneva, Graceful planes and lines, Theoret. Comput. Sci. 283 (1) (2002) 151–170.
[9] V.E. Brimkov, R.P. Barneva, Connectivity of discrete planes, Theoret. Comput. Sci. 319 (1–3) (2004) 203–227.
[10] V.E. Brimkov, R.P. Barneva, Plane digitization and related combinatorial problems, Discrete Appl. Math. 147 (2–3) (2005) 169–186.
[11] V.E. Brimkov, R.P. Barneva, On the polyhedral complexity of the integer points in a hyperball, Theoret. Comput. Sci. 406 (1–2) (2008) 24–30.
[12] V.E. Brimkov, R.P. Barneva, B. Brimkov, Connected distance-based rasterization of objects in arbitrary dimension, Graph. Models 73 (2011) 323–334.
[13] V.E. Brimkov, D. Coeurjolly, R. Klette, Digital planarity—A review, Discrete Appl. Math. 155 (4) (2007) 468–495.
[14] F. Chamizo, E. Cristobal, The sphere problem and the *L*-functions, Acta Math. Hungar. 135 (1–2) (2012) 97–115.
[15] F. Chamizo, E. Cristóbal, A. Ubis, Visible lattice points in the sphere, J. Number Theory 126 (2) (2007) 200–211.
[16] F. Chamizo, H. Iwaniec, On the sphere problem, Rev. Mat. Iberoam. 11 (2) (1995) 417–429.
[17] V. Chandru, S. Manohar, C.E. Prakash, Voxel-based modeling for layered manufacturing, IEEE Comput. Graph. Appl. 15 (6) (1995) 42–47.
[18] J.K. Cochran, Ceramic hollow spheres and their applications, Curr. Opin. Solid State Mater. Sci. 3 (5) (1998) 474–479.
[19] D. Cohen-Or, A. Kaufman, Fundamentals of surface voxelization, Graph. Models Image Process. 57 (6) (1995) 453–461.
[20] H.S.M. Coxeter, Regular Polytopes, Dover Publications, 1973.
[21] J.A. Ewell, Counting lattice points on spheres, Math. Intell. 22 (4) (2000) 51–53.

Please cite this article in press as: R. Biswas, et al., On the polyhedra of graceful spheres and circular geodesics, Discrete Applied Mathematics (2015), http://dx.doi.org/10.1016/j.dam.2015.11.017

[22] C. Fiorio, D. Jamet, J.-L. Toutant, Discrete circles: An arithmetical approach with non-constant thickness, in: A.Y.W. Longin Jean Latecki, David M. Mount, (Eds.), Vision Geometry XIV, Electronic Imaging, SPIE, vol. 6066, San Jose (CA), USA, 2006, p. 60660C.
[23] O. Fomenko, Distribution of lattice points over the four-dimensional sphere, J. Math. Sci. 110 (6) (2002) 3164–3170.
[24] J. Françon, On recent trends in discrete geometry in computer science, in: S. Miguet, A. Montanvert, S. Ubèda (Eds.), Discrete Geometry for Computer Imagery, in: Lecture Notes in Computer Science, vol. 1176, Springer, Berlin, Heidelberg, 1996, pp. 1–16.
[25] M. Ghahramani, A. Garibov, T. Agayev, Production and quality control of radioactive yttrium microspheres for medical applications, Appl. Radiat. Isot. 85 (2014) 87–91.
[26] L. Guo, X. Dong, X. Cui, F. Cui, J. Shi, Morphology and dispersivity modulation of hollow microporous spheres synthesized by a hard template route, Mater. Lett. 63 (13–14) (2009) 1141–1143.
[27] D.R. Heath-Brown, Lattice points in the sphere, in: Number theory in progress, Walter de Gruyter, Berlin, II:883–892, 1999.
[28] J. Hiller, H. Lipson, Design and analysis of digital materials for physical 3D voxel printing, Rapid Prototyp. J. 15 (2) (2009) 137–149.
[29] J. Hiller, H. Lipson, Tunable digital material properties for 3D voxel printers, Rapid Prototyp. J. 16 (4) (2010) 241–247.
[30] M. Kawashita, R. Shineha, H.-M. Kim, T. Kokubo, Y. Inoue, N. Araki, Y. Nagata, M. Hiraoka, Y. Sawada, Preparation of ceramic microspheres for in situ radiotherapy of deep-seated cancer, Biomaterials 24 (17) (2003) 2955–2963.
[31] O. Kim, Rapid prototyping of electrically small spherical wire antennas, IEEE Trans. Antennas and Propagation 62 (7) (2014) 3839–3842.
[32] R. Klette, A. Rosenfeld, Digital Geometry: Geometric Methods for Digital Picture Analysis, Morgan Kaufmann, San Francisco, 2004.
[33] H. Lipson, J.B. Pollack, Automatic design and manufacture of robotic lifeforms, Nature 406 (2000) 974–978.
[34] H. Maehara, On a sphere that passes through n lattice points, European J. Combin. 31 (2) (2010) 617–621.
[35] A. Magyar, On the distribution of lattice points on spheres and level surfaces of polynomials, J. Number Theory 122 (1) (2007) 69–83.
[36] C. Montani, R. Scopigno, in: A.S. Glassner (Ed.), Graphics gems (Chapter: Spheres-to-voxels conversion), Academic Press Professional, Inc., San Diego, CA, USA, 1990, pp. 327–334.
[37] D. Nain, M. Styner, M. Niethammer, J. Levitt, J.E. Shenton, M.G. Gerig, A. Bobick, A. Tannenbaum, Statistical shape analysis of brain structures using spherical wavelets, in: Proc. 4th IEEE International Symposium on Biomedical Imaging: From Nano to Macro, ISBI 2007, 2007, pp. 209–212.
[38] T. Nanya, H. Yoshihara, T. Maekawa, Reconstruction of complete 3D models by voxel integration, J. Adv. Mech. Des. Syst. Manuf. 7 (3) (2013) 362–376.
[39] B. Roget, J. Sitaraman, Wall distance search algorithm using voxelized marching spheres, in: 7th International Conference on Computational Fluid Dynamics. ICCFD7, 2012, pp. 1–23.
[40] B. Roget, J. Sitaraman, Wall distance search algorithm using voxelized marching spheres, J. Comput. Phys. 241 (2013) 76–94.
[41] F.F. Sene, J.R. Martinelli, E. Okuno, Synthesis and characterization of phosphate glass microspheres for radiotherapy applications, J. Non-Cryst. Solids 354 (42–44) (2008) 4887–4893.
[42] J.-L. Toutant, E. Andres, T. Roussillon, Digital circles, spheres and hyperspheres: From morphological models to analytical characterizations and topological properties, Discrete Appl. Math. 161 (16–17) (2013) 2662–2677.
[43] K.-M. Tsang, Counting lattice points in the sphere, Bull. Lond. Math. Soc. 32 (2000) 679–688.
[44] X. Zhang, J. Stockel, M. Wolf, P. Cathier, G. McLennan, E. Hoffman, M. Sonka, A new method for spherical object detection and its application to computer aided detection of pulmonary nodules in CT images, in: N. Ayache, S. Ourselin, A. Maeder (Eds.), Medical Image Computing and Computer-Assisted Intervention, MICCAI 2007, Springer, Berlin, Heidelberg, 2007, pp. 842–849.
[45] M. Zheng, J. Cao, X. Chang, J. Wang, J. Liu, X. Ma, Preparation of oxide hollow spheres by colloidal carbon spheres, Mater. Lett. 60 (24) (2006) 2991–2993.
[46] E. Zubko, D. Petrov, Y. Grynko, Y. Shkuratov, H. Okamoto, K. Muinonen, T. Nousiainen, H. Kimura, T. Yamamoto, G. Videen, Validity criteria of the discrete dipole approximation, Appl. Opt. 49 (8) (2010) 1267–1279.

Please cite this article in press as: R. Biswas, et al., On the polyhedra of graceful spheres and circular geodesics, Discrete Applied Mathematics (2015), http://dx.doi.org/10.1016/j.dam.2015.11.017